Research Article

Nano Biomed Eng

Immobilization of Thai Population-specific Human Leukocyte Antigens on Magnetic Nanoparticles Integrated with Nuclear Magnetic Resonance Technology

Wichai Subtaweewasin, Wanchai Pijitrojana

Department of Electrical and Computer Engineering, Thammasat School of Engineering, Thammasat University, Pathumthani, Thailand

Corresponding authors. E-mail: WichaiSubtaweewasin@gmail.com; Pwanchai@engr.tu.ac.th

Received: Dec. 30, 2022; **Revised:** Mar. 6, 2023; **Accepted:** Mar. 27, 2023

Citation: W. Subtaweewasin, W. Pijitrojana. Immobilization of Thai population-specific HLA on magnetic nanoparticles integrated with nuclear magnetic resonance technology. *Nano Biomedicine and Engineering*, 2023.

http://doi.org/10.26599/NBE.2023.9290009

Abstract

Kidney disease, as a global health problem, can progress to kidney failure. Kidney transplantation is a treatment option for end-stage disease and an alternative to dialysis. Complement-dependent cytotoxicity tests and flow cytometry are methods used to test for compatibility between autoantibodies and donor recipient. Antibodies against donor human leukocyte antigens (HLAs), linked to hyperacute or severely acute rejection, frequently result in graft loss. Currently, fluorescent bead assay (Luminex®) technology is used in Thailand for HLA–antibody typing tests. However, each test requires specific location and time, expensive equipment, and high costs. The goal of such research is that, HLA–antibody typing tests can be performed wherever it is the most convenient for recipients and hospitals. A further advantage is that the surgeon can perform a final test for confirmation before the surgery. Numerous technologies are currently available for this purpose. The focus of this study was on the Fe_3O_4 magnetic nanoparticles (MNPs) immobilized with HLAs frequently found in the Thai population. These were examined using nuclear magnetic resonance (NMR) to measure HLA antibody typing. MNPs have recently attracted considerable attention because of their strong magnetization and large surface areas. Immobilization reactions with antigens and the straightforward magnetic separation of MNPs are low-cost techniques. Hence, the commercialization of Fe_3O_4 MNPs is favorable. In this study, MNPs were functionalized with 3-aminopropyl triethoxysilane (APTES) in toluene and ethanol, and the nanoparticles were streptavidin activated after APTES treatment. A specific biotinylated HLA for the Thai population was used and immobilized on streptavidin. The MNPs were effectively immobilized. The magnetic properties can be modified by adding other ions to Fe_3O_4. We discovered that the shape and size variations of Fe_3O_4 MNPs may have an impact on the amount of functionalized and immobilized surface area.

Keywords: magnetic nanoparticles; human leukocyte antigen; micro-nuclear magnetic resonance; immobilization; human leukocyte antigens antibody; kidney transplantation

Introduction

Kidney disease (KD) is a significant global health problem. Recently, the number of people with renal illnesses has increased worldwide. Dialysis is the ultimate treatment for KD and helps patients extend their

lives. Chronic kidney disease (CKD) is the most prevalent factor leading to kidney (renal). The Thai Transplant Society requires patients to register for KT. Over time, the number of transplants has gradually increased. Kidneys are obtained from both live and deceased donors (LD and DD, respectively) [1–4]. Data indicate that the number of DD has increased at a greater rate than LD. Prior to surgery, transplant patients must take a blood test to determine if they match with the a LD or a DD. Kidney transplant recipients are divided into groups according to their age (if over 18) [2]. A blood test determines the tissue typing and ABO compatibility required for successful transplantation. The donor and recipient must share the same or compatible blood type.

Human leukocyte antigens (HLAs) and HLA antibodies are the essential components for the success of kidney transplantation. Before receiving a kidney transplant, a patient or recipient carrying donor-specific HLA antibodies (DSA) is at risk of experiencing HLA antibody-mediated rejection and kidney wasting [5–7]. Currently, a single antigen bead multiplex fluorescence-based solid-phase immunoassay (Luminex assay) with high sensitivity and specificity is used for the detection of antibodies recognized by HLA. However, this technique has the potential to produce false-positive and false negative results owing to variations in density, shape, and antigen on the microparticle beads. Dyed microparticle beads were used with the Luminex assay. A single-coated HLA bead is called a single-antigen bead (SAB). Owing to its excellent sensitivity and specificity, it can identify a particular serum in the recipient. The specificity of the antibody used in the Luminex assay is compared with the donor's HLA to determine whether the recipient carries DSA [8].

Nuclear magnetic resonance (NMR) technology is superior to existing techniques. Current methods for HLA detection are complement-dependent cytotoxicity (CDC), flow cytometry, and solid phase assays. These are more expensive and time-consuming than biosensor technologies. Currently, numerous biosensor technologies are available, including NMR, surface plasmonic resonance (SPR) [9–14,], and ion-sensitive field-effect transistor (ISFET) technology [8]. NMR has the potential to reduce the cost of testing and processing time required for HLA antibody typing tests. Some individuals forego the HLA antibody typing procedure because of financial hardships. Using NMR technology, testing costs can be reduced, enabling patients to obtain their HLA antibody results.

The first prototype of a micro-NMR device and/or magnetic nanoparticles (MNPs) antigen bead for the HLA antibody typing test, based on its prevalence in the Thai population, was developed in this study. Both small and large hospitals and community health centers can use this technology. Additionally, it lowers costs to the patient over the course of the normal testing process that occurs every three months. It also decreases the cost of the equipment, time, and samples used. In the Thai population, we identified the prevalence of HLA, MHC class I and II. HLA-A2, having the highest prevalence of MHC class I in the Thai population, was selected for this study. The MNP, Fe_3O_4, is considered due to its ability to direct a magnetic field, low toxicity, strong biocompatibility, and high relaxivity [16–19] in a biosensing system based on micro-NMR. Owing to the instability of iron in a strongly acidic environment, MNPs may shorten the lifespan of a material. Strong magnetic interactions between the particles lead to particle agglomeration, which reduces the surface energy and particle dispersion in aqueous solutions and matrices. A large surface area leads to limitations. The magnetic activity decreases if proteins and/or enzymes are exposed to these interfaces. When conducting an HLA antibody typing test, MNP beads should be highly sensitive, specific, and require minimal amounts of sample. To overcome these limitations, various techniques have been used to modify surfaces by loading them with additional target chemicals or biological components during or after the production process. These techniques increase the biocompatibility, dispersibility, and biodegradability of Fe_3O_4 MNPs on their surface. This study focused on directly functionalizing the surfaces of Fe_3O_4 MNPs with 3-aminopropyl triethoxysilane (APTES) to create amine (NH_2) groups that can bind to other biomolecules. Streptavidin-biotin technology, which employs biologically mediated immobilization, is one of the most examined and utilized methods. In this study, streptavidin (SA) had already been functionalized with an amine group and immobilized with HLA-A2, was activated before immobilization. MNPs are affected by both physical and chemical factors. Understanding the characteristics, chemical compositions, and distribution of functional groups on the surfaces was a goal of this study.

The techniques used to investigate these include Fourier-transform infrared spectroscopy (FTIR), scanning electron microscopy (SEM), energy dispersive spectroscopy (EDS), transmission electron microscopy (TEM), X-ray photoelectron spectroscopy (XPS), atomic force microscopy (AFM), vibrating sample magnetometry (VSM), X-ray diffraction (XRD), and thermal gravimetric analysis (TGA) [20].

Experimental

Materials

Bovine serum albumin (BSA), 0.01% phosphate buffer saline powder, sodium azide (NaN_3), 3-aminopropyl (PBS) triethoxysilane ($C_9H_{23}NO_3Si$) (APTES), glutaraldehyde solution (GA), ethanol (EtOH), toluene AR, iron II/III oxide (Fe_3O_4), 50–100 nm in particle diameter (97% trace metals basis), and SA were purchased from Sigma-Aldrich (USA). Biotin-labeled Pro5 MHC pentamer A 02:01(HLA-A2 antigen), and anti-HLA-A2 were purchased from Proimmune (UK). The uniform magnetic field for NMR was purchased from Dexing Magnet Tech Co., Ltd. (China).

Methods

Preparation of MNPs for micro-NMR detection

350 mg of Fe_3O_4 MNPs was sonicated in a mixture of EtOH and toluene (1:2 volume fraction). The Fe_3O_4 MNPs and APTES at ratios of 1:1, 1:2, and 1:3 were reacted at 25 °C and stirred for 4 h. The precipitate was dried in air at 25 °C after being thoroughly rinsed with ethanol several times until all residues had been removed, as indicated in Fig. 1.

SA coating of MNPs

The Fe_3O_4 MNP treatment with APTES included additional SA in two different concentrations (20 and 40 μg/mL). At 4 °C, the mixture was incubated for 20 h. Reconstituted SA-Fe_3O_4 MNPs were added to 0.2 mL of PBS (pH = 7.4) containing 1.0% BSA. Subsequently, samples were kept in a refrigerator for several days at 2–8 °C as shown in Fig. 1.

Immobilization of MNPs

Prior to use, the vortexed Fe_3O_4 MNPs/APTES/SA was mixed for 20 s. A suitable amount of Fe_3O_4 MNPs/APTES/SA was added to a tube along with one antigen test volume (10 μL) of biotin-labeled HLA antigen. The tube was incubated on ice for 30 min while being mixed. The tube volume was increased to 2 mL with wash buffer (NaN_3 and BSA), and the tube was then placed in a magnetic particle separator. After 3–5 min, the fraction containing the Fe_3O_4/APTES/SA MNPs:HLA antigen complexes was washed three times with buffer before use, as depicted in Fig. 1.

Characteristics of MNPs

FTIR

Data were obtained on a Nicolet iS50, Thermo

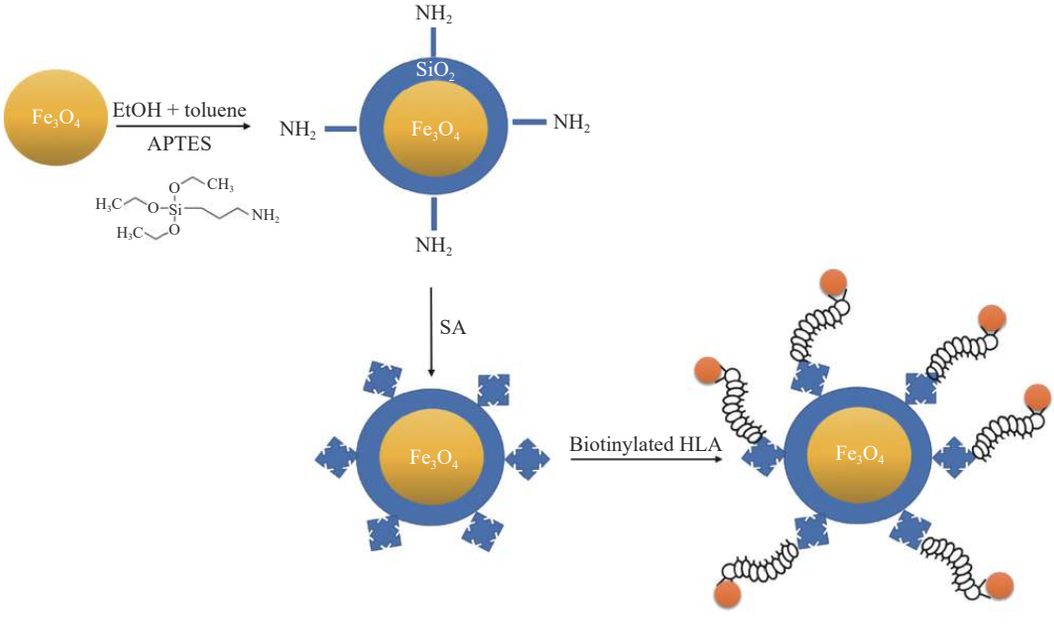

Fig. 1 Experimental preparation of MNPs.

Scientific. To perform the measurements, the sample was diluted with potassium bromide (KBr) and acquired over a range of 400–4 000 cm^{-1}.

Field emission scanning electron microscope (*FE-SEM*)

Data were obtained on a QUORUM Q150R ES using gold. The solid surface of the MNPs was determined using SEM. This SEM renders images in three-dimensional (3D) and is used to examine the morphology and specificity of the sample surface. Crystal alignment was checked using a backscattering electron diffraction-reception system. EDS was used to assess changes in the extracted sample. The SEM X-ray detector enabled analysis of the elements of the sample.

Vibrating sample magnetometer (*VSM*)

An in-house developed vibrating sample magnetometer (VSM, calibrated with a 3-mm-diameter Ni sphere, model 730908 LakeShore) was used. The instrument analyzes the magnetic characteristics of low-magnetic moments and nanostructured materials. To display a hysteresis curve, the magnetization of the sample is monitored, and the resonance frequency of the vibration-detection device is scanned.

Results and Discussion

Characteristics of functionalization and immobilization

FTIR spectroscopy

Figure 2 shows the FTIR spectra of the uncoated Fe_3O_4 and functionalized Fe_3O_4 with APTES-SA modified MNPs. The bands on the FTIR curve between 526 and 682 cm^{-1} are caused by Fe—O bonding in Fe_3O_4. As shown in Fig. 2(a), the Fe_3O_4 MNPs displayed a potent absorption band at approximately 537 cm^{-1}. In Fig. 2(b), the band at 3 334 cm^{-1} in the FTIR is related to the OH bond. The Fe_3O_4 MNPs are functionalized by coating their surface with APTES (Fe_3O_4:APTES) (1:3), which

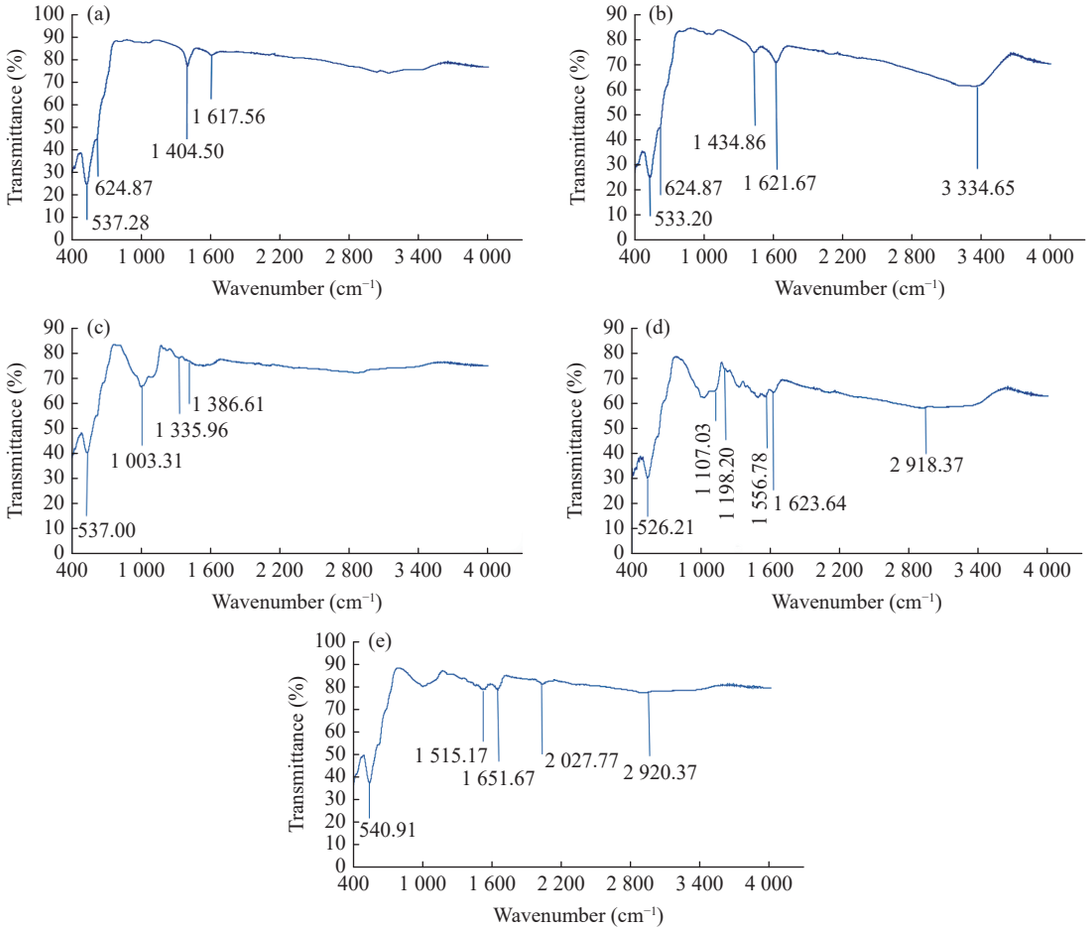

Fig. 2 FTIR spectra of MNPs at different processing steps. (**a**) Fe_3O_4; (**b**) Fe_3O_4+(EtOH-toluene); (**c**) Fe_3O_4+(EtOH-toluene)+APTES; (**d**) Fe_3O_4+(EtOH-toluene)+APTES+SA; (**e**) Fe_3O_4+(EtOH-toluene)+APTES +SA+HLA (biotin-labeled).

was selected because it showed the best. O—Si—O and Fe—Si occur as bands in the spectra at around 1 003 cm^{-1} in Fig. 2(c) and 1 107 cm^{-1} in Fig. 2(d), respectively, in symmetric stretching vibration. Figure 2(d) shows an amine group (N—H) band at 1 623 cm^{-1} on the surface. The vibration associated with the C—N group is located at approximately 1 198 cm^{-1}. Figure 2(d) shows the spectrum of the functionalized SA at a wavelength of around 1 556 cm^{-1}. The FTIR spectrum of Fe_3O_4/APTES/SA/HLA is displayed in Fig. 2(e). Figure 2(e) shows the amide group spectrum of the MHC class I antigen, HLA-A2. At 1 651 cm^{-1}, a protein-helix peak was seen [21]. These results demonstrate the effectiveness of functionalization and immobilization.

SEM

Fe_3O_4 MNPs from a commercial source are depicted in Fig. 3(a), having various sizes and shapes with 50–100 nm in diameter. For functionalization and immobilization, the form and size of magnetic nanoparticles are crucial. Figure 2(a) shows different sizes and shapes of Fe_3O_4 with a flat surface, which may affect how another molecule can adhere to the surface. The MNPs were spherical. Biomolecules aggregate better on smooth regions of MNPs rather than on bumpy and rough surfaces. Figure 3(b) shows the silanization of MNP with APTES on their uneven surfaces. The distribution of free amine groups (NH_2) may be affected by the disruption and clumping of the APTES molecules on the surface of the MNPs. The shapes of the MNPs changed after functionalization with SA, as shown in Figs. 3(c) and 3(d). The SA at 20 μg had more pronounced agglomeration on the surface than at 40 μg. The density of biomolecules on the MNP surface was evident in the morphology of the MNPs/APTES/SA (20 μg), as illustrated in Fig. 3(c). In Fig. 3(d), the surface of MNPs functionalized with SA at 40 μg exhibits results comparable to those of SA at 20 μg, but with less density than other surfaces. Biotin-labeled HLA antigens were immobilized at both SA concentrations.

Magnetic measurements

The magnetic characteristics of the Fe_3O_4 MNPs were measured by VSM. The hysteresis loops of the four samples are displayed in Fig. 4. In comparison to the other samples, Fe_3O_4+APTES (60.07 emu/g), Fe_3O_4+APTES+SA (61.14 emu/g), and Fe_3O_4+APTES+SA+HLA (65.29 emu/g), Fe_3O_4 exhibits the highest saturation magnetization of 68.80 emu/g at room temperature. In this figure, the retention and coercivity are not zero for all APTES modifications, APTES modifications plus SA, and APTES modifications plus SA plus HLA. A soft

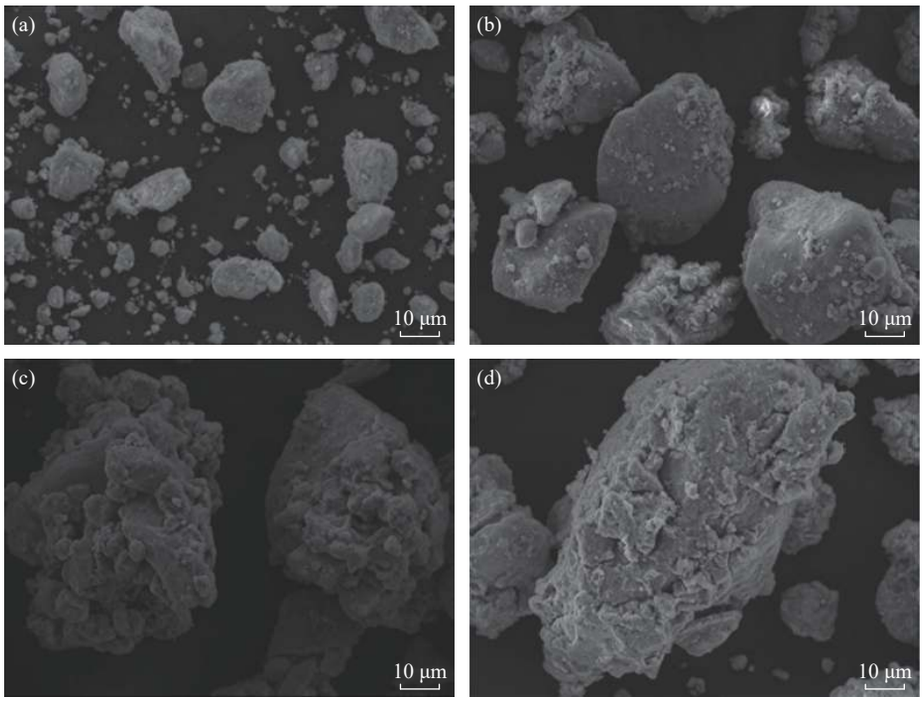

Fig. 3 SEM images of MNPs during each processing step. (**a**) Fe_3O_4; (**b**) Fe_3O_4+(EtOH-toluene)+APTES; (**c**) Fe_3O_4+(EtOH-toluene)+APTES+SA (20 μg/mL); (**d**) Fe_3O_4+(EtOH-toluene)+APTES+SA (40 μg/mL).

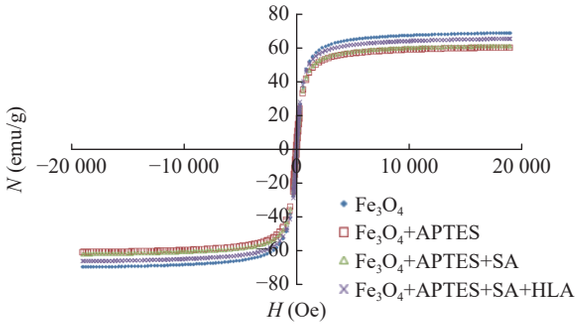

Fig. 4 Hysteresis loops of the four samples. Magnetization curves of Fe_3O_4, Fe_3O_4+APTES, Fe_3O_4+APTES+SA, and Fe_3O_4+APTES+SA+HLA.

ferromagnetic material (Fe_3O_4) with a small coercive force is shown for all the samples in Fig. 4. Surface modification of the Fe_3O_4 MNPs and coated SiO_2 shells may be responsible for the variation in the saturation magnetization values. These traits describe superparamagnetic Fe_3O_4 NPs in general.

EDX analysis from EDS

Figure 5 shows the EDX spectrum of Fe_3O_4 MNPs functionalized with APTES and SA at concentrations of 20 and 40 μg/mL containing carbon (C), chlorine (Cl), oxygen (O), silicon (Si), and iron (Fe) elements. The EDX spectrum composed of C (5.06), O (32.93), Si (1.06), and Fe (60.95) is completely functionalized with APTES and SA (20 μg/mL).

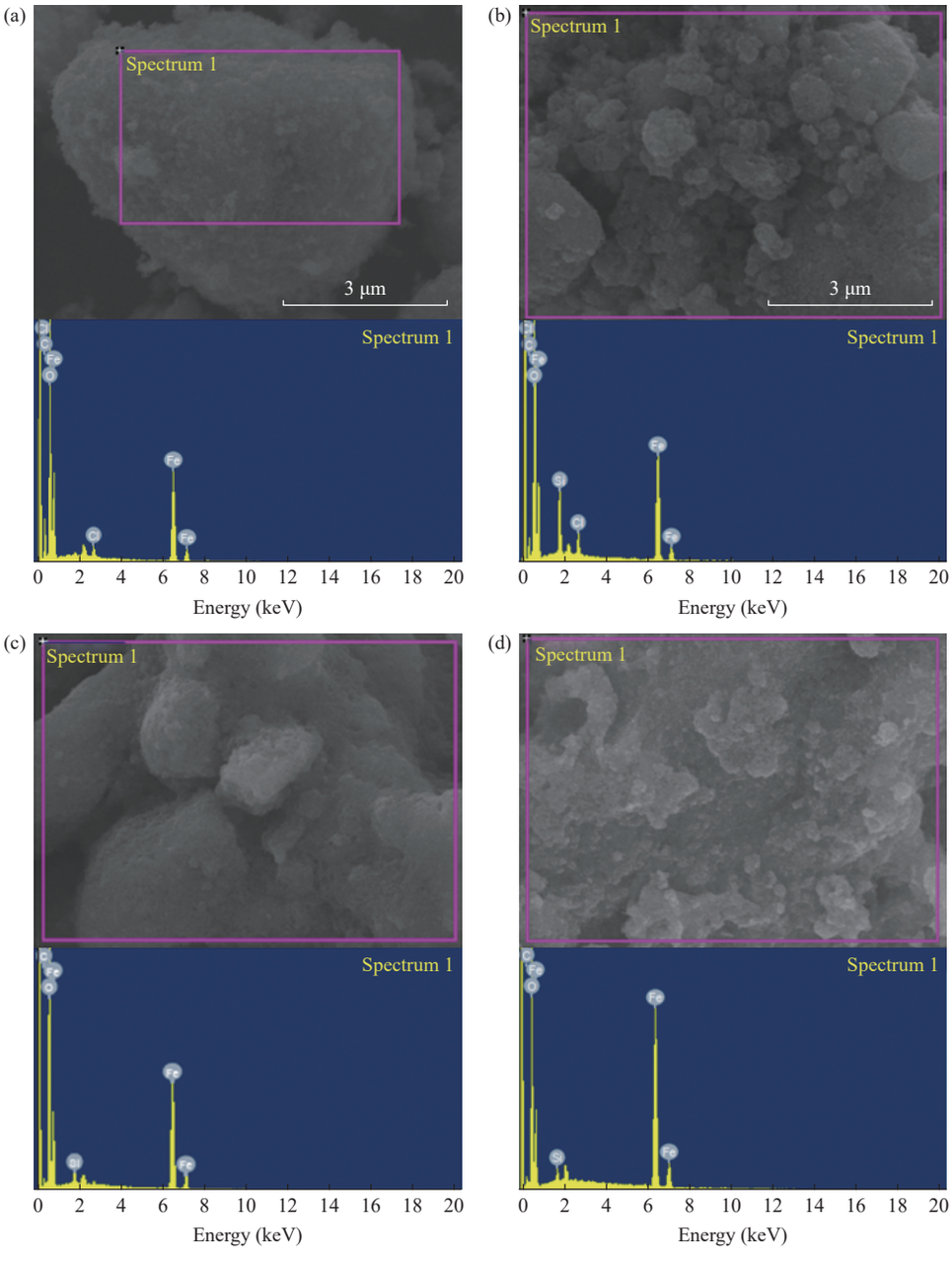

Fig. 5 Elements in (**a**) Fe_3O_4; (**b**) Fe_3O_4+(EtOH+toluene)+APTES; (**c**) Fe_3O_4+(EtOH+toluene)+APTES+SA (20 μg/mL); (**d**) Fe_3O_4+(EtOH+toluene)+APTES+SA (40 μg/mL).

Conclusion

The HLA-A2 antigen, occurring in the highest frequency specific to the Thai population, was immobilized on Fe_3O_4 MNPs. Using silanization, the Fe_3O_4 MNP surface was functionalized with APTES to produce MNPs containing amino groups with a specific Fe_3O_4:APTES ratio. The amino groups of APTES aid in the surface functionalization of SA on the MNPs. During immobilization, the modified MNPs aggregated with HLA-A2 biotin-labeled MNPs. The surface properties of the modified MNPs improved as a result of APTES functionalization. The structure of Fe_3O_4 MNPs with APTES was confirmed by FTIR to have an amine group, and SA and HLA antigens were effectively immobilized. The approach of preparing and modifying Fe_3O_4 MNPs with APTES in the appropriate ratio results in the desired qualities with SA at different concentrations. It triggers the collection of biotin-labeled HLA antigens. FTIR indicates that MHC class I, HLA-A2 includes a significant amount of α-helix. The magnetic properties can be modified by adding other ions to Fe_3O_4. In our investigation, we discovered that the shape and size variations of Fe_3O_4 MNPs may have an impact on the amount of functionalized and immobilized surface area. In subsequent studies, we will assess the sensitivity and specificity of our custom-built micro-NMR with specific antibodies to HLA antigens using this MNP.

CRediT Author Statement

Wichai Subtaweewasin performed conceptualization, investigation, methodology, the experiments, data analyzing, and manuscript preparation. **Wanchai Pijitrojana** supervised and counselled.

Acknowledgement

The author would like to thank the National Research Council of Thailand (NRCT) and Thammasat School of Engineering, Thammasat University for a research grant.

Conflict of Interest

The authors declare that no competing interest exists.

References

[1] N. Larpparisuth, W. Cheungpasitporn, A. Lumpaopong. Global perspective on kidney transplantation: Thailand. *Kidney360*, 2021, 2(7): 1163−1165. https://doi.org/10.34067/KID.0002102021

[2] P. Rianthavorn. 2019 Annual Report of Organ Transplantation in Thailand. Thai Transplantation Society, 2019.

[3] P. Kupatawintu, S. Pheancharoen, A. Srisuddee, et al. HLA-A, -B, -DR haplotype frequencies in the Thai stem cell donor registry. *Tissue Antigens*, 2010, 75(6): 730−736. https://doi.org/10.1111/j.1399-0039.2010.01450.x

[4] S. Ounjai, P. P., S. Kanunthong, A. Srisuddee, et al. HLA-A, -B, and -DR frequencies in deceased kidney donors from the Organ Donation Center Thai Red Cross Society. *Journal of Hematology and Transfusion Medicine*, 2019, 29: 175–181. (in Thai)

[5] B.H. Chung, Y.Y. Joo, J. Lee, et al. Impact of ABO incompatibility on the development of acute antibody-mediated rejection in kidney transplant recipients presensitized to HLA. *PLoS One*, 2015, 10(4): e0123638. https://doi.org/10.1371/journal.pone.0123638

[6] B. Clark, D.J. Unsworth. HLA and kidney transplantation. *Journal of Clinical Pathology*, 2010, 63(1): 21−25. https://doi.org/10.1136/jcp.2009.072785

[7] E. Lougee, S. Morjaria, O. Shaw, et al. A new approach to HLA typing designed for solid organ transplantation: Epityping and its application to the HLA-a locus. *International Journal of Immunogenetics*, 2013, 40(6): 445−452. https://doi.org/10.1136/jcp.2009.072785

[8] B.D. Tait. Detection of HLA antibodies in organ transplant recipients-triumphs and challenges of the solid phase bead assay. *Frontiers in Immunology*, 2016, 7: 570. https://doi.org/10.3389/fimmu.2016.00570

[9] G. Wang, C. Wang, R. Yang, et al. A sensitive and stable surface plasmon resonance sensor based on monolayer protected silver film. *Sensors*, 2017, 17(12): E2777. https://doi.org/10.3390/s17122777

[10] J.T. Liu, P.S. Lin, Y.M. Hsin, et al. Surface plasmon resonance biosensor for microalbumin detection. *Journal of the Taiwan Institute of Chemical Engineers*, 2011, 42(5): 696−700. https://doi.org/10.1016/j.jtice.2011.01.005

[11] H. Ahn, H. Song, J.R. Choi, et al. A localized surface plasmon resonance sensor using double-metal-complex nanostructures and a review of recent approaches. *Sensors*, 2017, 18(1): E98. https://doi.org/10.3390/s18010098

[12] N. Kostevšek. A review on the optimal design of magnetic nanoparticle-based T_2 MRI contrast agents. *Magnetochemistry*, 2020, 6(1): 11. https://doi.org/10.3390/magnetochemistry6010011

[13] O.V. Shynkarenko, S.A. Kravchenko. Surface plasmon resonance sensors: Methods of surface functionalization and sensitivity enhancement. *Theoretical and Experimental Chemistry*, 2015(5): 273. https://doi.org/10.1007/s11237-015-9427-5

[14] L.A. Lyon, M.D. Musick, M.J. Natan. Colloidal Au-enhanced surface plasmon resonance immunosensing. *Analytical Chemistry*, 1998, 70(24): 5177−5183. https://doi.org/10.1021/ac9809940

[15] A. Dupré, K.M. Lei, P.I. Mak, et al. Micro- and nanofabrication NMR technologies for point-of-care medical applications–A review. *Microelectronic Engineering*, 2019. 209: 66–74. https://doi.org/10.1016/j.mee.2019.02.005

[16] Y. Liu, N. Sun, H. Lee, et al. CMOS mini nuclear magnetic resonance system and its application for biomolecular sensing. In: *Proceedings of 2008 IEEE International Solid-State Circuits Conference*, 2008. https://doi.org/10.1109/isscc.2008.4523096/mm1

[17] Y. Sahoo, A. Goodarzi, M.T. Swihart, et al. Aqueous ferrofluid of magnetite nanoparticles: fluorescence labeling and magnetophoretic control. *The Journal of Physical Chemistry B*, 2005, 109(9): 3879−3885. https://doi.org/10.1021/jp045402y

[18] Y. Mizukoshi, S. Seino, K. Okitsu, et al. Sonochemical preparation of composite nanoparticles of Au/gamma-Fe_2O_3 and magnetic separation of glutathione. *Ultrasonics Sonochemistry*, 2005, 12(3): 191−195. https://doi.org/10.1016/j.ultsonch.2003.12.003

[19] V.M. Costa, M.C.M. de Souza, P.B.A. Fechine, et al. Nanobiocatalytic systems based on lipase-Fe_3O_4 and conventional systems for isoniazid synthesis: A comparative study. *Brazilian Journal of Chemical Engineering*, 2006, 33: 661−673. https://doi.org/10.1590/0104-6632.20160333s20150137

[20] J.K. Xu, J.J. Sun, Y.J. Wang, et al. Application of iron magnetic nanoparticles in protein immobilization. *Molecules*, 2014, 19(8): 11465−11486. https://doi.org/10.3390/molecules190811465

[21] J.C. Gorga, A. Dong, M.C. Manning, et al. Comparison of the secondary structures of human class I and class II majors histocompatibility complex antigens by Fourier transform infrared and circular dichroism spectroscopy. *Proceedings of the National Academy of Sciences*, 1989, 86(7): 2321−2325. https://doi.org/10.1073/pnas.86.7.2321

[22] N. Gunawansa, R. Rathore, A. Sharma, et al. Crossmatch strategies in renal transplantation: A practice guide for the practicing clinician. *Journal of Transplant Surgery*, 2017, 1(1): 8−15. https://doi.org/10.36959/338/325

[23] S. Ferrari-Lacraz, J.M. Tiercy, J. Villard. Detection of anti-HLA antibodies by solid-phase assay in kidney transplantation: Friend or foe. *Tissue Antigens*, 2012, 79(5): 315−325. https://doi.org/10.1111/j.1399-0039.2012.01853.x

[24] H.Y. Song, J. Hobley, X. Su, et al. End-on covalent antibody immobilization on dual polarization interferometry sensor chip for enhanced immuno-sensing. *Plasmonics*, 2014, 9(4): 851−858. https://doi.org/10.1007/s11468-014-9680-9

[25] N.K. Mehra, A.K. Baranwal. Clinical and immunological relevance of antibodies in solid organ transplantation. *International Journal of Immunogenetics*, 2016, 43(6): 351−368. https://doi.org/10.1111/iji.12294

[26] R.J. Duquesnoy, M. Marrari. Correlations between terasaki's HLA class I epitopes and HLAMatchmaker-defined eplets on HLA-A, -B and-C antigens. *Tissue Antigens*, 2009, 74(2): 117−133. https://doi.org/10.1111/j.1399-0039.2009.01271.x

[27] J.M. Greene, R.W. Wiseman, S.M. Lank, et al. Differential MHC class I expression in distinct leukocyte subsets. *BMC Immunology*, 2011, 12: 39. https://doi.org/10.1186/1471-2172-12-39

[28] P. Molek, T. Bratkovič. Epitope mapping of mono- and polyclonal antibodies by screening phage-displayed random peptide libraries. *Acta Chimica Slovenica*, 2016, 63(4): 914−919. https://doi.org/10.17344/acsi.2016.2458

[29] A. Man-Kupisinska, M. Michalski, A. Maciejewska, et al. A new ligand-based method for purifying active human plasma-derived ficolin-3 complexes supports the phenomenon of crosstalk between pattern-recognition molecules and immunoglobulins. *PLoS One*, 2016, 11(5): e0156691. https://doi.org/10.1371/journal.pone.0156691

[30] C.S.M. Kramer, D.L. Roelen, S. Heidt, et al. Defining the immunogenicity and antigenicity of HLA epitopes is crucial for optimal epitope matching in clinical renal transplantation. *HLA*, 2017, 90(1): 5–16. https://doi.org/10.1111/tan.13038

[31] N. Sun, Y. Liu, H. Lee, et al. CMOS RF biosensor utilizing nuclear magnetic resonance. *IEEE Journal of Solid-State Circuits*, 2009, 44(5): 1629−1643. https://doi.org/10.1109/jssc.2009.2017007

[32] M. Ylmaz, C. Ozic, I. Gok. Principles of nucleic acid separation by agarose gel electrophoresis. In: *Gel Electrophoresis—Principles and Basics*, 2012. https://doi.org/10.5772/38654

[33] K.M. Lei, P.I. Mak, M.K. Law, et al. A palm-size μNMR relaxometer using a digital microfluidic device and a semiconductor transceiver for chemical/biological diagnosis. *The Analyst*, 2015, 140(15): 5129−5137. https://doi.org/10.1039/c5an00500k

[34] Y.L. Luo, E.C. Alocilja. Portable nuclear magnetic resonance biosensor and assay for a highly sensitive and rapid detection of foodborne bacteria in complex matrices. *Journal of Biological Engineering*, 2017, 11: 14. https://doi.org/10.1186/s13036-017-0053-8

[35] S. Sabban, H.T. Ye, B. Helm. Development of an *in vitro* model system for studying the interaction of *Equus caballus* IgE with its hight-affinity FcεRI receptor. *Jounrnal of Visualized Experiments*, 2014, 93: e52222. https://doi.org/10.3791/52222

[36] A.K. Gupta, R.R. Naregalkar, V.D. Vaidya, et al. Recent advances on surface engineering of magnetic iron oxide nanoparticles and their biomedical applications. *Nanomedicine*, 2007, 2(1): 23−39. https://doi.org/10.2217/17435889.2.1.23

[37] K.S. Park, H. Kim, S. Kim, et al. Nanomagnetic system for rapid diagnosis of acute infection. *ACS Nano*, 2017, 11(11): 11425−11432. https://doi.org/10.1021/acsnano.7b06074

[38] H.Y. Lin, C.H. Huang, J. Park, et al. Integrated magneto-chemical sensor for on-site food allergen detection. *ACS Nano*, 2017, 11(10): 10062−10069. https://doi.org/10.1021/acsnano.7b04318

[39] Y. Luo, E.C. Alocilja. Portable nuclear magnetic resonance biosensor and assay for a highly sensitive and rapid detection of foodborne bacteria in complex matrices. *Journal of Biological Engineering*, 2017, 11: 14. https://doi.org/10.1186/s13036-017-0053-8

[40] A.C. Barreto, F.J.N. Maia, V.R. Santiago, et al. Novel ferrofluids coated a renewable material obtained from cashew nut shell liquid. *Microfluidics and Nanofluidics*, 2011, 12(5): 677−686. https://doi.org/10.1007/s10404-011-0910-6

[41] Can, K., Ozmen, M., Ersoz, M. Immobilization of albumin on aminosilane modified superparamagnetic magnetite nanoparticles and its characterization. *Colloids and Surfaces B*, *Biointerfaces*, 2009, 71(1): 154−159. https://doi.org/10.1016/j.colsurfb.2009.01.021

[42] J.S. Choi, S. Kim, D. Yoo, et al. Distance-dependent magnetic resonance tuning as a versatile MRI sensing platform for biological targets. *Nature Materials*, 2017, 16(5): 537−542. https://doi.org/10.1038/NMAT4846

[43] J.T. Jang, H. Nah, J.H. Lee, et al. Critical enhancements of MRI contrast and hyperthermic effects by dopant-controlled magnetic nanoparticles. *Angewandte Chemie*, 2009, 48(7): 1234−1238. https://doi.org/10.1002/ange.200805149

[44] A. Cavalli, X. Salvatella, C.M. Dobson, et al. Protein structure determination from NMR chemical shifts. *Proceedings of the National Academy of Sciences of the*

United States of America, 2007, 104(23): 9615−9620. https://doi.org/10.1073/pnas.0610313104

[45] R. Li, F. Feng, Z.Z. Chen, et al. Sensitive detection of carcinoembryonic antigen using surface plasmon resonance biosensor with gold nanoparticles signal amplification. *Talanta*, 2015, 140: 143−149. https://doi.org/10.1016/j.talanta.2015.03.041

[46] N. Gunawansa, R. Rathore, A. Sharma, et al. Crossmatch strategies in renal transplantation: A practical guide for the practicing clinician. *Journal of Transplant Surgery*, 2017, 1(1): 8−15. https://doi.org/10.1016/j.talanta.2015.03.041

[47] B.D. Tait. Detection of HLA antibodies in organ transplant recipients–triumphs and challenges of the solid phase bead assay. *Frontiers in Immunology*, 2016, 7: 570. https://doi.org/10.3389/fimmu.2016.00570

[48] W.A. Talavera-Pech, A. Esparza-Ruiz, P. Quintana-Owen, et al. Effects of different amounts of APTES on physicochemical and structural properties of amino-functionalized MCM-41- MSNs. *Journal of Sol-Gel Science and Technology*, 2016, 80(3): 697−708. https://doi.org/10.1007/s10971-016-4163-4

[49] S. Sajjadifar, Z. Gheisarzadeh. Isatin-SO_3H coated on amino propyl modified magnetic nanoparticles (Fe_3O_4@APTES@isatin-SO_3H) as a recyclable magnetic nanoparticle for the simple and rapid synthesis of pyrano[2,3-d] pyrimidines derivatives. *Applied Organometallic Chemistry*, 2018, 33(1): e4602. https://doi.org/10.1002/aoc.4602

[50] B.T. Thanh, N. Van Sau, H. Ju, et al. Immobilization of protein A on monodisperse magnetic nanoparticles for biomedical applications. *Journal of Nanomaterials*, 2019, 2019: 1−9. https://doi.org/10.1155/2019/2182471

[51] B. Thangaraj, Z. Jia, L. Dai, et al. Effect of silica coating on Fe_3O_4 magnetic nanoparticles for lipase immobilization and their application for biodiesel production. *Arabian Journal of Chemistry*, 2016, 12(8): 4694−4706. https://doi.org/10.1016/j.arabjc.2016.09.004

[52] J.K. Xu, J.J. Sun, Y.J. Wang, et al. Application of iron magnetic nanoparticles in protein immobilization. *Molecules*, 2014, 19(8): 11465−11486. https://doi.org/10.3390/molecules190811465

[53] S.F. Chew, B.R. Wood, C. Kanaan, et al. Fourier transform infrared imaging as a method for detection of HLA class I expression in melanoma without the use of antibody. *Tissue Antigens*, 2007, 69(Suppl 1): 252−258. https://doi.org/10.1111/j.1399-0039.2006.00775.x

[54] J.K. Xu, J.J. Sun, Y.J. Wang, et al. Application of iron magnetic nanoparticles in protein immobilization. *Molecules*, 2014, 19(8): 11465−11486. https://doi.org/10.3390/molecules190811465